

Spectral Characteristics of Segmented Optical Waveguides Immersed in a Fluid Medium

José Rodríguez García* and Adrián Fernández Gavela

Abstract—In this paper, the electromagnetic scattering properties due to periodical configurations consisting of planar optical waveguides completely surrounded by a fluid media, in gaseous or liquid phase, are analyzed. In this new design, fluid separates the consecutive optical waveguides, and it is also the common cover for all of them, thus significantly increasing the effect of the fluid on the evanescent field. This new configuration is designated as fluidic segmented optical waveguides. The theoretical algorithm was developed and recently updated by the authors, and it is based on the generalized scattering matrix concept, together with the generalized telegraphist equations formalism and modal matching technique. We present the first theoretical results concerning to these periodical structures with a fluidic common cover. To carry out the simulations, with the purpose to manufacture these devices in the future, glass and polymer were chosen as materials for the optical waveguides substrate and for enclosing the fluid as common cover medium, respectively. The spectral results obtained for the module and phase of the reflection and transmission coefficients have shown great sensitivity of the new proposal to the variations of the refractive index of the fluid, making it very attractive for the design of refractive index sensors and optical biosensors.

1. INTRODUCTION

Light flow control is a very powerful strategy in the design of integrated optical devices. The worlds of health, environment, communications and research are and will be great beneficiaries of the technology capable of controlling and applying light in micro and nanometric scales. An example is the field of optical detection, where among other proposals, interferometry [1–4] and periodic structures [5–9] have played a very important role. On the other hand, the combination of liquids and light has given rise to the optofluidics field, which has generated interesting technological contributions and improvements in light sources, sensing applications as well as in tunable and reconfigurable optical devices [10–13].

In former contributions [14, 15], the authors have developed, computed and verified a theoretical procedure that allows to know the electromagnetic scattering properties of arbitrary dielectric waveguides connected in cascade, both abruptly and gradually. The Generalized Scattering Matrix (GSM) concept, together with the Generalized Telegraphist Equations (GTE) formalism and Modal Matching Technique (MMT) are the theoretical foundations on which the complete algorithm is based. The good efficiency of the theoretical procedure was demonstrated by comparing the theoretical values with the experimental results, both at microwave and optical frequencies.

Integrated planar optical waveguides and closed microchannels in cascade were analyzed by the authors in a previous work [15]. In the present contribution, we are interested in periodic arrangements of planar optical waveguides completely surrounded by a fluid media (gaseous or liquid), so that the optical waveguides in cascade are separated by fully open successive fluid regions. The regions containing fluid were designed by means of microchannels engraved on the substrate and connected to each other

Received 27 November 2018, Accepted 30 January 2019, Scheduled 5 February 2019

* Corresponding author: Jose Rodriguez Garcia (jose@uniovi.es).

The authors are with the Physics Department, University of Oviedo, Oviedo, Asturias 33007, Spain.

on the common cover of the optical waveguides. Consequently, in this new design, fluid separates the consecutive optical waveguides, and it is also the common cover for all planar optical waveguides. With the physical structure, we design this new configuration as fluidic segmented optical waveguides. The core of this proposal is significantly increasing the influence of the fluid on the evanescent field which reaches the optical waveguides cover medium. In this way, both planar interfaces (waveguides-fluid) and evanescent field in the waveguides cover medium contribute to the final behaviour of the device, significantly increasing its sensitivity in order to be used as refraction index sensors and optical biosensors.

We present the first theoretical results concerning these periodical structures with a fluidic common cover. In order to implement these devices for experimental evaluation in the future, glass and polymer were chosen as materials for the optical waveguides substrate and for enclosing the fluid in the common cover region, respectively. Fluidic segmented optical waveguides, with different numbers of microchannels and different refractive indices of the fluid, were analyzed. The spectral results obtained for the module and phase of the reflection and transmission coefficients have shown the great sensitivity of the new proposal, both versus the number of microchannels and the variations in the fluid refractive index, making it very attractive for the design of refractive index sensors and optical biosensors.

2. THEORY

Initially, the complete mathematical algorithm was developed by the authors in order to analyze periodic structures between dielectric waveguides at microwave and optical frequencies [14]. The theoretical results were confirmed experimentally, and they demonstrated the possibility of obtaining a wide range of devices; for example, electromagnetic and photonics band gaps, power dividers, optical switches and optical microcavities can be designed based on the physical characteristics of the periodic structures.

In this first version of the method, the cover medium of the waveguides was air. However, in order to analyze the influence of the cover refraction index on the behavior of the device, the procedure was reformulated and computed, so that at the present time, any refractive index can be used as optical waveguide cover. The accuracy of the new version of the method was theoretically verified in its application to the analysis of 1-D photonic crystals and planar optical waveguides separated by closed microchannels in cascade [15]. The results obtained allowed to predict the possibility of designing refractive index sensors and optical biosensors based on the simultaneous action of two contributions: a) the interaction of the evanescent field with the waveguide cover medium, b) the electromagnetic dispersion at the perpendicular interfaces to the flow of the light.

The aforementioned update was explained in detail in [14, 15], and it can be summarized as follows:

The new refraction index profile of an integrated planar optical waveguide with a cover medium different to air, as shown in Figure 1(a), can be written in the form:

$$n(y) = \begin{cases} n_c, & \text{cover} \\ n_s + \Delta n \cdot f\left(-\frac{y}{h}\right), & \text{core} \\ n_s, & \text{substrate} \end{cases} \quad (1)$$

where n_s is the refractive index of the optical waveguide substrate; Δn refers to the maximum refractive index increment in the core region; f represents the refraction index function along y direction; h is the diffusion depth; and n_c refers to the refraction index of an hypothetical medium (solid, liquid or gaseous) as waveguide cover. The function f modulates the refraction index from waveguide surface ($y = 0$) to h , where the core ends. In the most general cases, the refraction index is gradual, with the maximum value at $y = 0$ and decreasing towards $y = h$. Exponential, Gaussian and complementary error are the most common f functions. This is the case for integrated optical waveguides fabricated by ion/proton-exchange and diffusion, which are the techniques that we generally use in our laboratory. In our model, the graded refraction index in the core is simulated by using a dynamic mesh of pixels which makes possible the analysis of any gradual function f . Consequently, arbitrary fine meshes can be used in order to optimize the core refractive index function. Boundary conditions of perfectly conduction walls are applied, as shown in Figure 1(a).

The electromagnetic scattering properties in periodic configurations of dielectric waveguides, as shown in Figure 1(b), are evaluated following two well-differentiated steps developed by the authors

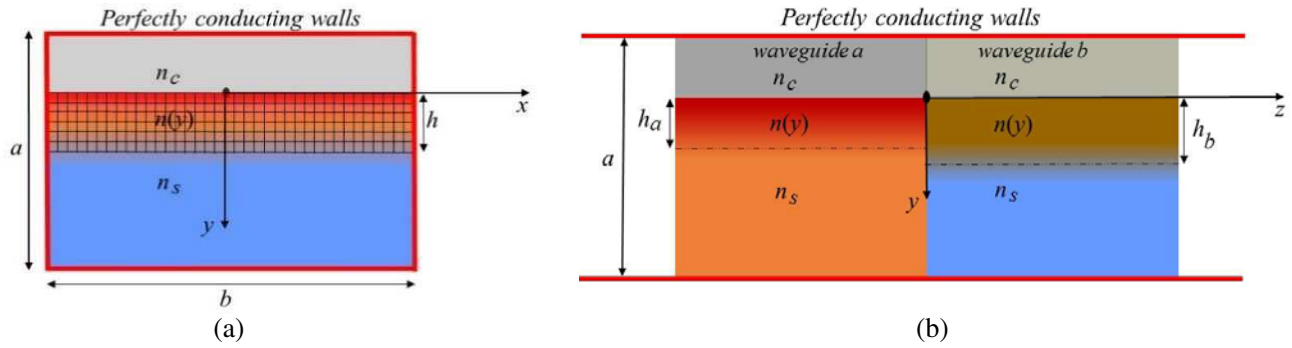


Figure 1. (a) Cross section of a planar optical waveguide modelled by a grid of pixels and with boundary conditions of perfectly conducting walls. (b) Two planar optical waveguides connected by an abrupt transition.

and described in [14, 15]:

a) Optical waveguides proper modes analysis: GTE formulation provides surface, fast and evanescent proper modes solutions.

b) GSM evaluation of single and multiple discontinuities: MMT procedure and a matrix connection algorithm provide the GSM of the complete structure.

As explained in detail by the authors [14, 15], from the Helmholtz’s equation, expanding the electromagnetic field of the proper modes as a series of orthogonal functions (basic modes) and applying perfectly conductive boundary conditions, the GTE formulation provides the optical waveguides proper modes. Subsequently, the MMT procedure allows calculating the scattering matrix of each simple discontinuity. Finally, a matrix connection technique is applied to determine the total generalized scattering matrix corresponding to a cascade set of discontinuities, as shown in Figure 2.

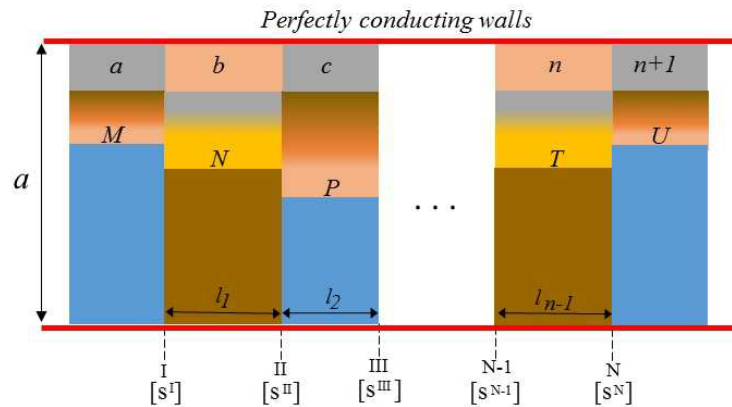


Figure 2. General representation of a cascaded set of N abrupt discontinuities in shielded dielectric waveguides.

The generalized scattering matrix, once organized, has the following structure:

$$[S^T] = \begin{bmatrix} [S_{11}^T (M \times M)] & [S_{12}^T (M \times U)] \\ [S_{21}^T (U \times M)] & [S_{22}^T (U \times U)] \end{bmatrix} \quad (2)$$

where $[S_{ij}^T]$ ($i = 1, 2; j = 1, 2$) are complex submatrices, while subscripts i and j represent the reception proper modes and the incidence proper modes, respectively. The complex elements of the GSM are the reflection and transmission coefficients (modulus and phase) between proper modes, and they give

the electromagnetic behaviour of the complete structure under analysis. To perform the new spectral analysis, the reformulated algorithm was implemented in the updated software package *Telcont* [15].

3. EXPERIMENTAL PROPOSAL

Recently, the authors have analyzed the electromagnetic properties of periodical structures consisting of planar optical waveguides in cascade separated by microchannels [15]. In the referenced work, the microchannels were engraved in soda-lime microscope glass slides using laser lithography and wet etching techniques. The complete fabrication process has been performed in a clean room of our laboratory and involved a controlled protocol of successive steps, as explained in [16]. Later, the microchannels were individually closed by using polymer as waveguides cover medium.

Soda-lime glass, whose physical properties are well known [17], is composed of abundant and inexpensive materials: about 70 percent of silicon dioxide, 15 percent of sodium oxide, 9 percent of calcium oxide, and amounts of various other compounds. At visible wavelengths, this glass has a transmittance of 90% and refractive index values in the interval (1,511–1,538), which makes it very attractive for optical applications. With respect to the polymer, PDMS was chosen as the cover material for optical waveguides and for sealing the microchannels. The adhesion forces between PDMS and glass provide an excellent bounding between polymer and optical waveguide surface as well as a perfect sealing of the microchannels. In addition, the PDMS polymer can be removed and repositioned on the glass as many times as required. Both materials offer a low dispersion of refractive index at visible wavelengths.

It was demonstrated that the refraction index of the analyte strongly influences both the evanescent field in the waveguides cover and the electromagnetic scattering at the interfaces waveguide-microchannel-waveguide. According to the obtained results, the authors have concluded that refractive index sensors and optical biosensors could be designed via these two simultaneous effects: evanescent field and scattering.

For this reason and in order to increase the sensitivity of the sensor as well as to simplify its fabrication, in this work we propose a new periodical configuration denominated fluidic segmented optical waveguides. In the new design, planar optical waveguides are completely surrounded by a fluid medium, and the fluid separates the consecutive optical waveguides and also as the common cover for all of them. In this way, the effect of the fluid on the evanescent field in the waveguide cover medium is significantly increased.

Figure 3 shows the new design, such that the fluid, in addition to separating the guides, becomes the common cover. The fluid flows perpendicularly to the light propagation direction.

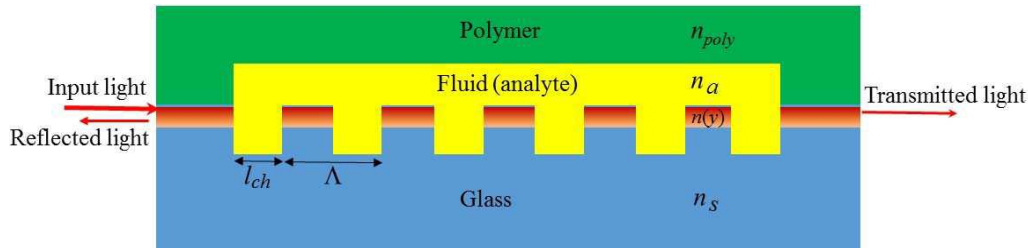


Figure 3. Side view of a periodical configuration in segmented optical planar waveguides completely surrounded by a fluid media. In this case, the periodicity are provided by 5 segmented planar optical waveguides in cascade which connect the input optical waveguide with the output optical waveguide. The common cover is a fluid enclosed by 6 interconnected microchannels.

For evaluating the spectral performance of the new purposed device, we have designed two configurations of fluidic segmented optical waveguides. To explore both the influence of the microchannels number and the refractive index of the analyte on the transmission and reflection properties, devices with 7 and 15 microchannels have been analyzed. In all cases and in order to reduce the number of parameters, the width, l_{ch} , and period, Λ , of the microchannels remained constant. The physical parameters were as follows: conducting walls cross section dimensions, $(a \times b)$: $(35 \times 60) \mu\text{m}$;

basic modes number: 80; proper modes number: $M = N = P = \dots = 15$; substrate refraction index (glass), $n_s = 1.512$, maximum index increment: $\Delta n = 0.01$; diffusion depths (μm): $h = 2$; index profile functions of planar waveguides: Gaussian; waveguide lengths (μm): 50; period of the microchannels (μm): $\Lambda = 100$; PDMS polymer cap, for covering the microchannels and as cover medium only for input and output optical waveguides: $n_{poly} = 1.42$; refraction indices of analyte in the microchannels and in the common cover medium: n_a . The optical waveguides are single-mode.

In order to fabricate and characterize the device experimentally, this new design offers several advantages. On the one hand, the materials are glass (soda lime) and polymer (PDMS). As mentioned, these materials are very cheap, easy to handle and offer low dispersion of refractive index at visible wavelengths. On the other hand, as all the channels are open at the top, unlike the former design, the alignment of the set of microchannels with the polymer cap is much simpler and more precise. The fabrication process will be carried out in our laboratory and involves the following stages:

a) Single-mode planar optical waveguide fabrication by means of ion-exchange and diffusion in soda lime glass substrate. This process is very well controlled in our lab.

b) Manufacture of the mask to replicate the microchannels to be engraved in the soda lime substrate. This process will be carried out in a clean room using the laser lithography system implemented in our laboratory.

c) A mask is used for UV irradiation of the fabricated optical planar waveguide, which was previously coated with a specific photoresist.

d) Photoresist development and manufacture of the microchannels by means of wet etching, with a hydrofluoric acid dissolution.

e) Fabrication of the PDMS polymer cap, positioning and alignment on the microchannels.

Figure 4 shows the experimental setup in order to verify the performance of the device. The main modules of the optical experimental arrangement will consist of a tunable laser, an optical circulator, and an optical analyzer. To inject the fluid, a fluid delivery system must be added.

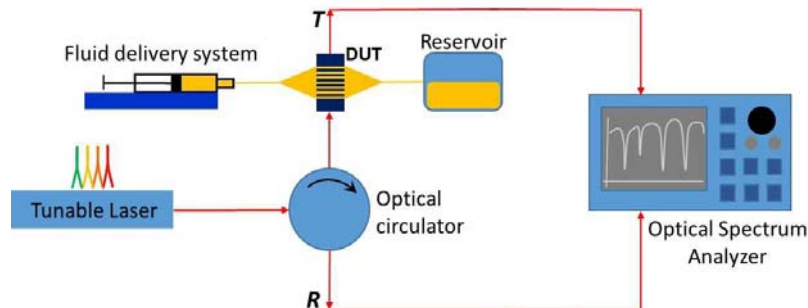


Figure 4. Experimental assembly for the spectral characterization of segmented optical waveguides surrounded by a fluidic medium.

Finally, it will be very interesting to analyze the behaviour of these periodical structures taking as parameter the duty cycle, γ , defined as l_{ch}/Λ . In addition to the refractive index of both the optical waveguides and the fluid, there are other critical parameters: the length of the microchannels, l_{ch} , the period of the microchannels, Λ , as well as the waveguide lengths, which play very important roles in the final behavior of the periodical structure. These tasks are planned for the future.

4. RESULTS

In order to analyze in depth the reflection and transmission characteristics of these new periodical arrangements, spectral results were obtained for devices susceptible of being manufactured in our laboratory.

Figure 5 shows and compares the modulus of the reflection, R , and transmission, T , coefficients for the fundamental proper mode, for two devices of fluidic segmented optical waveguides with 7 and

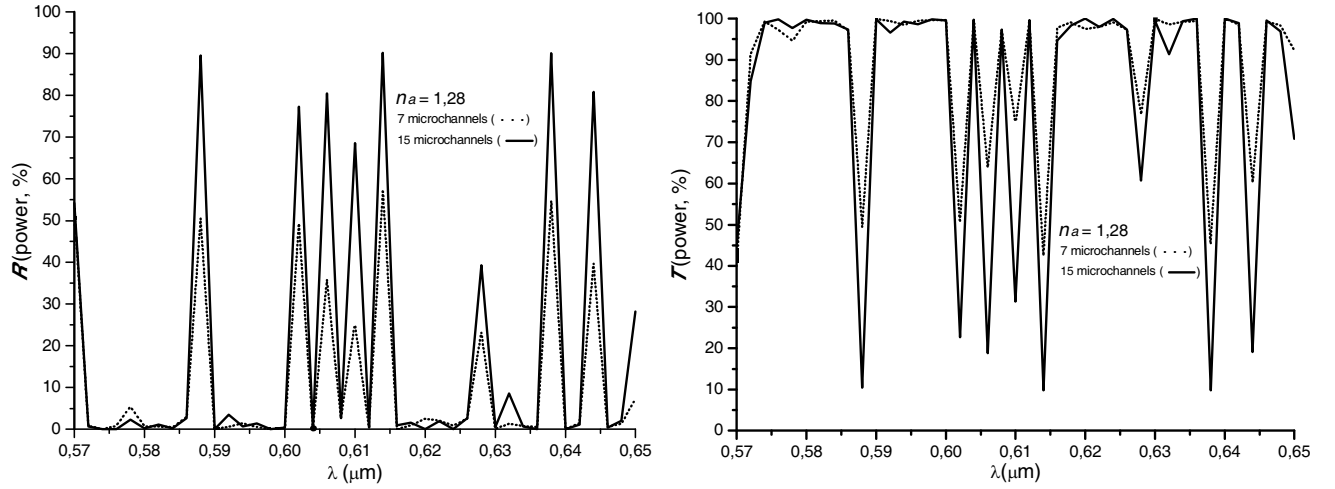


Figure 5. Modulus of the reflection, R , and transmission, T , coefficients for single-mode fluidic segmented optical waveguides with 7 and 15 microchannels and refractive index of the analyte, $n_a = 1.28$.

15 microchannels. In both cases, the refractive index of the analyte, $n_a = 1.28$. It can be seen that by doubling the number of microchannels, the reflection is doubled, and transmission is halved. The strong reflections and transmissions are maintained at the same wavelengths, regardless of the number of microchannels. Therefore, the number of microchannels affects fundamentally the magnitude of reflection and transmission, but not the wavelength where strong variations occur. In other words, once refractive indices are set, the strong reflection and transmission effects depend on the number of microchannels, occurring at the same wavelengths, for any number of microchannels. The total power is conserved, as can be deduced when comparing the reflected and transmitted power percentages.

In order to analyze the sensitivity of the device when refractive index of the analyte is modified, we have simulated a fluidic segmented optical waveguide with 7 microchannels. As in the previous case, the simulations were carried out by using, as wavelength increment, $\Delta\lambda = 0.002 \mu\text{m}$. As already mentioned, the wavelengths for which strong reflections and transmissions are produced depend on the refractive index of the analyte, n_a . The results are shown in Figure 6 when $n_a = 1.24, 1.32, 1.40$, with $\Delta n_a = 0.08$. We see that as the refractive index of the analyte is increased, the reflection is reduced, while the transmission increases. This behaviour is because by increasing the refractive index of the analyte, a better adaptation of the wave impedance is achieved, which increases the transmission of the electromagnetic wave propagated by the periodic structure. The above is well appreciated comparing the results in Figures 6(a) and 6(b). In the case of $n_a = 1.24$, the wave impedance change in each guide-channel-guide interface is very strong, which translates into strong reflections; however, for the case of $n_a = 1.40$, this refractive index is close to the refractive index of the substrate ($n_s = 1.512$) and the guiding region, which favors the transmission. In all cases, the power conservation is excellent.

In order to confirm the previous results, a fluidic segmented optical waveguide has been designed with 15 microchannels. As in the case of 7 microchannels, it is observed that by increasing the refractive index of the analyte, the transmission is increased, while the reflection is reduced. This is seen very well in Figure 7, where the reflection and transmission are compared for two refractive indices of the analyte, $n_a = 1.28$ and $n_a = 1.36$. As shown in Figure 7(a), the periodicity of R and T coefficients is remarkable in the wavelengths range (0.60–0.616), when $n_a = 1.28$. Specifically, this periodicity is reflected and highlighted in Figure 7(b), resulting in a periodicity in the response of $\Delta\lambda = 0.004$ microns. Again, the conservation of the total power is excellent.

All previous simulations were performed using wavelengths increments $\Delta\lambda = 0.002 \mu\text{m}$. Therefore, it was decided to study this periodic behavior in the mentioned interval but using wavelengths increments $\Delta\lambda = 0.0001 \mu\text{m}$. The study was performed for the case of 15 microchannels and analyte refraction indices of 1.28 and 1.36. As shown in Figure 8, the peaks of reflection and transmission appear at different wavelengths for each refractive index; however, a periodicity of 1.3 nm is obtained in the responses (peaks) of reflection and transmission for both analyte refraction indices. Note that when

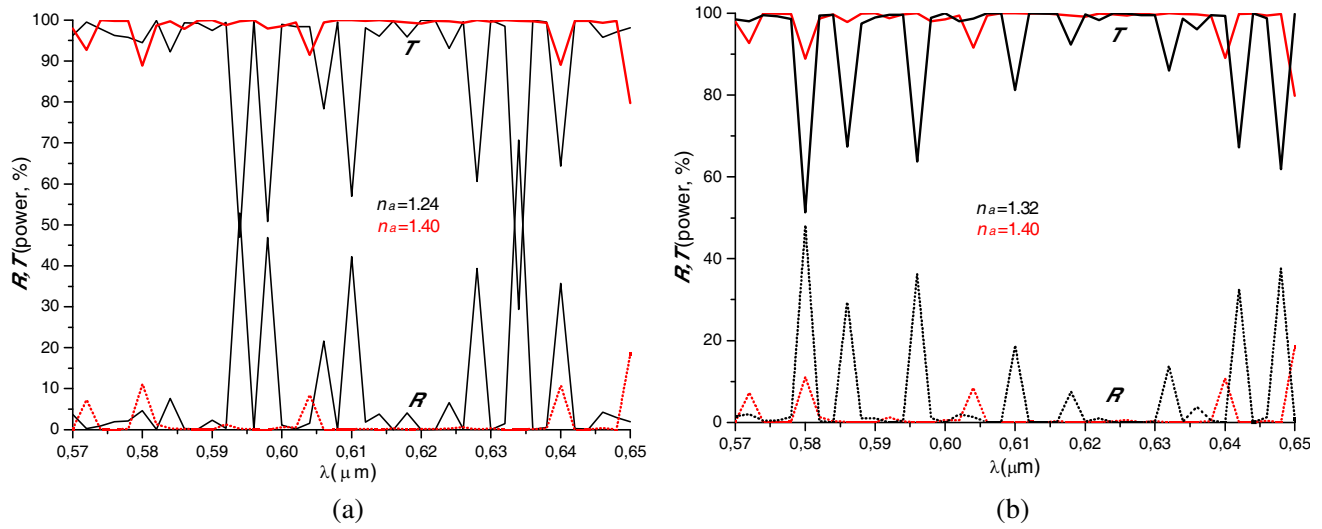


Figure 6. Modulus of the reflection, R , and transmission, T , coefficients for single-mode fluidic segmented optical waveguides with 7 microchannels and refractive index of the analyte, $n_a = 1.24$, 1.32 and 1.40 .

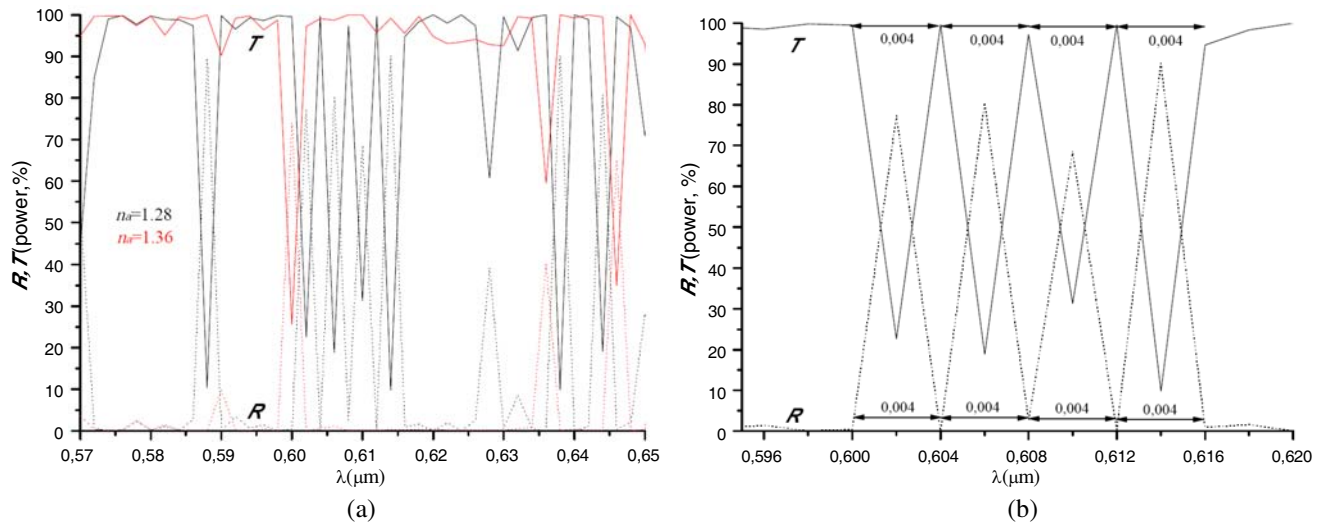


Figure 7. Modulus of the reflection, R , and transmission, T , coefficients for single-mode fluidic segmented optical waveguides with 15 microchannels and refractive index of the analyte, $n_a = 1.28$ and $n_a = 1.36$ in Figure 7(a). Figure 7(b) shows a periodicity of $\Delta\lambda = 0.004 \mu\text{m}$ for the R and T coefficients in the wavelengths range (0.60–0.616), when $n_a = 1.28$.

very small lambda increments ($\Delta\lambda = 0.0001 \mu\text{m}$) are chosen in the simulation, results are obtained that are not observed for the case of higher lambda increments ($\Delta\lambda = 0.002 \mu\text{m}$). This indicates the high sensitivity of the sensor structure, as well as the discrimination capacity of the mathematical algorithm responsible for the simulation.

So far only results of the module have been reported. With regard to the phase of the scattering parameters, in all the studied cases, a strong variation of the phase as a function of the wavelength is observed. As an example, Figure 9 shows the phase of the transmission coefficient for the case a fluidic segmented optical waveguide with 15 microchannels and refractive index of the analyte $n_a = 1.28$. These results were obtained for wavelength increments $\Delta\lambda = 0.0001 \mu\text{m}$. Double periodicity (gray and white zones) can be seen in the phase response for transmission.

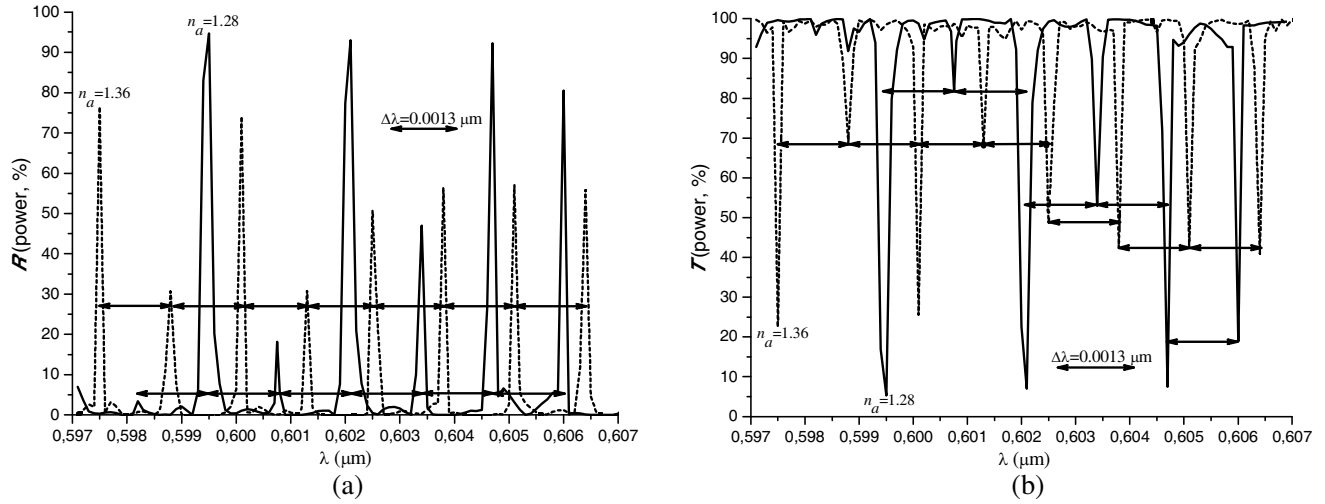


Figure 8. Peaks of reflection, R (a), and transmission, T (b), for a single-mode fluidic segmented optical waveguides with 15 microchannels and two refractive indices of the analyte, $n_a = 1.28$ and 1.36 . Wavelength increment of $\Delta\lambda = 0.0001 \mu\text{m}$ was used in the simulation.

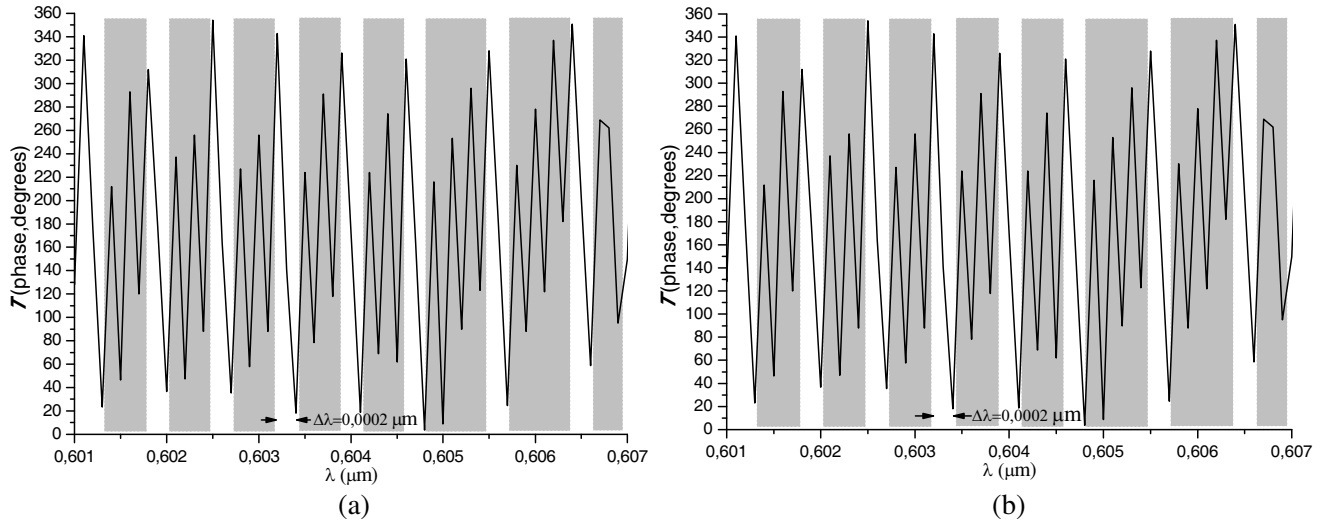


Figure 9. Phase of the transmission coefficient, T , for a fluidic segmented optical waveguide with 15 microchannels and refractive indices of the analyte $n_a = 1.28$ (a) and $n_a = 1.36$ (b). Double periodicity can be seen in the phase response for transmission.

The number of phase peaks in the gray region increases as the analyte index decreases, as can be deduced from Figure 9. We see that for $n_a = 1.28$ there are 4 and 5 phase jumps in the gray region, while for $n_a = 1.36$ there are 3 and 4 phase peaks in that region. It is important to point out that the consecutive gray periodic zones are separated $\Delta\lambda = 0.0003 \mu\text{m}$ and $\Delta\lambda = 0.0002 \mu\text{m}$ for $n_a = 1.28$ and $n_a = 1.36$, respectively. Consequently, it seems to be inferred that as the analyte index increases, the number of maximum and minimum (peaks) of phase in each gray periodic region is reduced; however, the number of gray periodic regions increases. In our case, this is already appreciated for a refraction index variation of 0.08. This result can be very interesting for sensing tasks, by detecting both the number of phase jumps (peaks) in the gray periodic regions and the total number of said periodic regions in the analyzed wavelength range.

5. CONCLUSIONS

The generalized scattering matrix concept, together with the generalized telegraphist equations formulism and modal matching technique can be applied for analyzing fluidic segmented optical waveguides. In these new structures, the simultaneous action of the planar interfaces and the evanescent field in the waveguides cover medium increase notably the sensitivity of periodical arrangements. Two configurations of fluidic segmented optical waveguides were studied in depth. The obtained results shown that the number of microchannels affects fundamentally the magnitude of reflection and transmission, but not the wavelength where strong variations occur. On the other hand, as the refractive index of the analyte increases, within the range of values that ensures guided single mode propagation, a better adaptation of the wave impedance is obtained, which justifies the reduction of the reflection and the increase of the transmission. The good discrimination capacity of the mathematical algorithm, for small variations of wavelength, allowed to verify that these periodical structures offers a great sensitivity both wavelength and refractive index variations. With regard to the phase of the scattering parameters, a strong variation was noticed as function of the wavelength, such that double periodicity appears in the phase response for the transmission coefficient. The obtained phase results allow thinking that the phase parameter will play an important role in the sensing processes. This is an advantage of these structures for sensing applications, by offering four sensing parameters: two modules and two phases. The fabrication and experimental evaluation of fluidic segmented optical waveguides will be two challenges of the future. In conclusion, the spectral results obtained for the module and phase of the reflection and transmission coefficients have shown the great sensitivity of the new proposal, both versus the number of microchannels and the variations in the fluid refractive index, making it very attractive for the design of refractive index sensors and optical biosensors.

ACKNOWLEDGMENT

This work has been supported by the University of Oviedo, under Project PAPI-17-PEMERG-9, and by the Spanish Government, under Project MINECO: CTQ2017-86994-R.

REFERENCES

1. Lal, S., et al., "Nano-optics from sensing to waveguiding," *Nature Photonics*, Vol. 1, 641–648, 2007.
2. Qi, Z., et al., "A design for improving the sensitivity of a Mach-Zehnder interferometer to chemical and biological measurands," *Sensors and Actuators B*, Vol. 8, 254–258, 2002.
3. McDonagh, C., et al., "Optical chemical sensors," *Chemical Reviews*, Vol. 108, 400–422, 2008.
4. Dante, S., et al., "All-optical phase modulation for integrated interferometric biosensors," *Optic Express*, Vol. 20, No. 7, 7195–7205, 2012.
5. Skivesen, N., et al., "Photonic-crystal waveguide biosensor," *Optic Express*, Vol. 15, No. 6, 3169–3176, 2007.
6. Nunes, P. S., et al., "Refractive index sensor based on a 1D photonic crystal in a microfluidic channel," *Sensors*, Vol. 10, 2348–2358, 2010.
7. Konopsky, V. N., et al., "Photonic crystal biosensor based on optical surface waves," *Sensors*, Vol. 13, 2566–2578, 2013.
8. Ramanujam, N. R., et al., "Enhanced sensitivity of cancer cell using one dimensional nano composite material coated photonic crystal," *Microsystem Technologies*, 1–8, 2018.
9. Taya, S. A., et al., "Photonic crystal with epsilon negative and double negative materials as an optical sensor," *Optical and Quantum Electronics*, Vol. 50, No. 5, 222-1–222-11, 2018.
10. Fainman, Y., D. Psaltis, L. P. Lee, and Ch. Yang, *Optofluidics: Fundamentals, Devices, and Applications*, McGraw-Hill Companies, Inc., 2010.
11. Monat, C., et al., "Integrated optofluids: A new river of light," *Nature Photonics*, Vol. 1, 106–113, 2007.

12. Erickson, D., et al., “Nanofluidic tuning of photonic crystals circuits,” *Proc. of SPIE*, Vol. 6475, 647513(1–11), 2007.
13. Luchansky, M. S. and R. C. Bailey, “High-Q optical sensors for chemical and biological analysis,” *Anal. Chem.*, Vol. 84, 793–821, 2012.
14. Rodríguez, J., et al., “Electromagnetic waves scattering at interfaces between dielectric waveguides: a review on analysis and applications,” *Progress In Electromagnetics Research B*, Vol. 37, 103–124, 2012.
15. Rodríguez, J. and A. F. Gavela, “Spectral behaviour of planar optical waveguides and microchannels in cascade: Theoretical evaluation,” *Progress In Electromagnetics Research M*, Vol. 72, 1–11, 2018.
16. Álvarez, M. C., et al., “Critical points in the fabrication of microfluidic devices on glass substrates,” *Sensors and Actuators B*, Vol. 130, 436–448, 2008.
17. Synowicki, R. A., et al., “Optical properties of soda-lime float glass from spectroscopic ellipsometry,” *Thin Solid Films*, Vol. 519, 2907–2913, 2011.